Intensity fluctuation spectroscopy of charged Brownian particles: the coherent scattering function

1978 J. Phys. A: Math. Gen. 11 119

(http://iopscience.iop.org/0305-4470/11/1/014)

J. Phys. A: Math. Gen., Vol. 11, No. 1, 1978. Printed in Great Britain.

Intensity fluctuation spectroscopy of charged Brownian particles: the coherent scattering function

P N Pusey

Royal Signals and Radar Establishment, Malvern, Worcs, WR14 3PS, UK

Received 29 July 1977

Abstract. We present measurements, which span wide ranges of scattering vector K and delay time τ, of the coherent intermediate scattering function $F(K, \tau)$ for a dispersion of strongly-interacting charged Brownian particles (radius ~ 250 Å). Emphasis is on the long-time decay of $F(K, \tau)$, i.e. for $\tau \gg \tau_I$, where $\tau_I (\sim 10^{-4}$ s) is the particle 'collision time'. D_L, the diffusion coefficient describing this long-time decay, was found to be several times smaller than D_0, the free-particle diffusion coefficient, and to be only weakly dependent on K. We argue that, for $K > K_{max}$, the position of the main peak in the particle structure factor $S(K)$, $F(K, \tau) \approx F_S(K, \tau)$, the self-scattering function which describes single-particle motions. We then conclude that the velocity autocorrelation function of a single particle has a weak but long-lived negative tail due to the repulsive interactions. Other theories relevant to the problem are reviewed briefly. An extended discussion is also given of the effects of multiple scattering in these and other experiments.

1. Introduction

Recent measurements (Brown *et al* 1975b) of the angular dependence of the intensity of light scattered by dispersions of charged colloidal particles at low ionic strengths yielded structure factors, $S(K)$, and radial distribution functions, $g(r)$; (here K is the scattering vector and r the interparticle spacing). These were similar in form to those obtained for dense atomic liquids by x-ray or neutron diffraction, indicating considerable short-range ordering of the colloidal particles due to repulsive shielded electrostatic interactions, with a spatial scale comparable to λ, the light wavelength. Study of the time dependence of fluctuations in the scattered laser light (intensity fluctuation spectroscopy) provides information on the motions of the particles in the dispersion. Here we report the first measurements of the temporal correlation function of the scattered light (related to the coherent intermediate scattering function $F(K, \tau)$), which span wide ranges of correlation delay time τ and scattering vector K.

An important timescale in the system is the 'collison time' τ_I, the time taken by a particle to move a reasonable fraction of the mean interparticle spacing. For times very much shorter than τ_I, the dominant influence in moving the particles is the strong rapidly fluctuating force due to collisions with the solvent molecules. (This force gives rise to the usual 'free-particle' Brownian motion.) To date, experiments have concentrated on this short-time region and reasonable agreement between experiment and theory has been found (see § 2). For $\tau \gtrsim \tau_I$, the weaker but longer-lived particle–particle forces become important leading to interactive motions of the particles. It is this longer-time region which forms the main subject of this paper. Typically τ_I is of the order of 10^{-4} s. This is in the middle of the range of times

(0 to $\sim 10^{-7}$ s) covered by photon correlation, intensity fluctuation techniques, which therefore provide a useful method for studying the transition from the 'free-particle' region, $\tau \ll \tau_I$, to the 'interactive' region, $\tau \geq \tau_I$.

In the next section we provide a more detailed review of past experiment and theory, expanding on the brief comments of the previous paragraph. Section 3 describes the experimental details, the data analysis and the results. It was found that, for $\tau \gg \tau_I$, the scattering function $F(K, \tau)$ was well represented by a single exponential in τ for K both less than and greater than K_{max}, the position of the main peak in $S(K)$. The diffusion coefficient associated with this longer-time behaviour was several times smaller than the free-particle diffusion coefficient and was only weakly dependent on scattering vector K. In § 4 we discuss sources of experimental error and uncertainty which include sample polydispersity, the presence in the samples of particulate contaminants of undetermined origin and multiple scattering. The discussion of multiple scattering (§ 4.3) is quite detailed, with assessments of its effect in earlier experiments as well as the present one. We suggest that, while the short-time decay of $F(K, \tau)$ can be severely distorted by multiple scattering, the long-time behaviour is relatively unaffected.

In § 5 the results are discussed. No theory for the complete behaviour of $F(K, \tau)$ appears to exist at present. In § 5.1 we make one or two general comments on both the short- and long-time behaviours. In § 5.2 we argue that, for $K > K_{max}$, the dominant contribution to $F(K, \tau)$ comes from single-particle correlations so that a measurement of $F(K, \tau)|_{K>K_{max}}$ can be regarded as an estimate of the self-scattering function $F_S(K, \tau)$. Then, by exploiting the similarity with incoherent neutron scattering by simple liquids, we conclude that the velocity autocorrelation function of a single particle has a weak but long-lived negative tail. A particle can be thought of as moving in a continuously evolving repulsive 'cage' formed by its neighbours. Thus two self-diffusion coefficients describe single-particle motions: the free-particle diffusion coefficient D_0 for times $\tau \ll \tau_I$, and, for $\tau \gg \tau_I$, a diffusion coefficient which is several times smaller than D_0 because of the hindering effects of the repulsive interactions. In § 5.3 we speculate briefly on the long-time behaviour of the coherent function $F(K, \tau)$. Section 5.4 is devoted to a brief review of other theoretical attempts to treat Brownian motion in interacting systems.

2. Review of previous work

2.1. Theory

The discussion will be limited to spherical particles. Under the conditions of these experiments intensity fluctuation spectroscopy provides a measure of $c^{1/2}|g^{(1)}(K, \tau)|$, where $g^{(1)}(K, \tau)$ is the normalised temporal autocorrelation function of the complex analytic field of the light scattered at wavevector K. Here c is a constant of order one for a given experiment, determined by such factors as spatial coherence of the scattered light at the detector, and $K \equiv (4\pi/\lambda)n \sin(\theta/2)$, where λ is the light wavelength *in vacuo*, n the refractive index of the supporting liquid and θ is the scattering angle. If it is assumed that the particles all have the same size (i.e. that they are monodisperse) and that the scattering is weak enough that the first Born approximation can be applied, then

$$|g^{(1)}(K, \tau)| = F(K, \tau)/S(K), \tag{1}$$

where the coherent intermediate scattering function $F(K, \tau)$ is given by

$$F(K, \tau) \equiv N^{-1} \sum_{i=1}^{N} \sum_{j=1}^{N} \langle \exp[i\boldsymbol{K} \cdot (\boldsymbol{r}_i(t) - \boldsymbol{r}_j(t+\tau))] \rangle \tag{2}$$

and the structure factor $S(K)$ by

$$S(K) \equiv F(K, 0). \tag{3}$$

Here N is the number of particles in the scattering volume and $\boldsymbol{r}_i(t)$ the position of particle i at time t. $S(K)$ is most easily obtained by separate measurements of the time-averaged scattered intensity. (For non-interacting particles $S(K) = 1$.) The radial distribution functions $g(r)$ can be obtained by numerical Fourier transformation of $S(K)$ (Brown *et al* 1975b).

Our main concern here is the functional form of $F(K, \tau)$. For non-interacting particles (e.g. low particle concentration, moderate electrolyte concentration where interparticle interactions are shielded) it is straightforward to show that (e.g. Cummins and Pusey 1977)

$$F(K, \tau) \equiv F_S(K, \tau) = \exp(-D_0 K^2 \tau) \tag{4}$$

where $F_S(K, \tau)$ is the self-(or incoherent) intermediate scattering function (§ 5.2) and D_0 is the 'free-particle' diffusion coefficient. It was argued in a previous paper (Pusey 1975) that, in the presence of long-range interactions, two types of force act on a particle: a strong, rapidly fluctuating 'Brownian force' due to the solvent molecules and a weaker, but longer-lived 'interaction force' due to the interparticle Coulombic forces. (As before we assume that the dominant effect of the small counter-ions is simply to determine the form of the shielded Coulombic interparticle potential; see, however, Harris (1976).) These forces, in turn, give rise to two components of the particle velocity: a Brownian component V_B with large mean-square value fluctuating on a timescale $\tau_B \approx 10^{-10}$ s and an interaction 'drift velocity' component V_I with much smaller mean-square magnitude fluctuating on timescale $\tau_I \approx 10^{-4}$ s. In terms of this model, with one or two additional assumptions, it can easily be shown that (Pusey 1975)

$$F(K, \tau)|_{\tau_B \ll \tau \ll \tau_I} = S(K) - D_0 K^2 \tau + \cdots \tag{5}$$

so that the initial decay of $|g^{(1)}(K, \tau)|$ (equation (1)) is given by

$$\frac{d}{d\tau}|g^{(1)}(K, \tau)|\Big|_{\tau_B \ll \tau \ll \tau_I} \equiv \frac{d}{d\tau} \ln|g^{(1)}(K, \tau)|\Big|_{\tau_B \ll \tau \ll \tau_I} = -D_{\text{eff}} K^2 \tag{6}$$

where

$$D_{\text{eff}} \equiv D_0 / S(K). \tag{7}$$

Thus the initial decay of $|g^{(1)}(K, \tau)|$ depends on the interaction only through the time-averaged structure $S(K)$. The analogy between this result and 'de Gennes narrowing' in neutron scattering has been pointed out by Pusey (1975) and Ackerson (1976).

Previously (Pusey 1975) it was perhaps not emphasised strongly enough that this derivation of equations (6) and (7) neglects hydrodynamic interactions, the effects on the motion of one particle of disturbances in the solvent set up by other particle motions (see, however, Ackerson 1976, 1977, Harris 1976). At the low volume

fractions, less than about 10^{-3}, typically used in these experiments this neglect would certainly be justifiable if the particles did not interact directly. Even in the presence of direct interactions the effect is probably small.

Equations (6) and (7) have also been derived independently by Ackerson (1976) and Berne (1977) (see § 5.4), and a more detailed discussion of the assumptions inherent in the derivation has been given by Harris (1976).

2.2. Experiment

Three different systems with Coulombic interactions have been studied by intensity fluctuation techniques in regions where $S(K)$ shows significant K dependence. Experiments by Pusey *et al* (1972) and Schaefer and Berne (1974) on the spherical virus R17 (radius ~ 140 Å) showed the inverse dependence of D_{eff} on $S(K)$ predicted by equations (6) and (7), though the value of D_{eff} was somewhat lower than predicted, possibly because of disruption of the virus particles at low ionic strength. Brown *et al* (1975b) studied polystyrene spheres of radius around 250 Å and found reasonable agreement with the theory over wide ranges of K vector and dispersion concentration. (Significant structure was found in a dispersion with a mean interparticle separation of nearly 20 particle diameters.) Schaefer and Ackerson (1975) reported measurements on polystyrene spheres of radius about 500 Å near a 'melting transition' from a solid-like to a liquid-like arrangement of particles. Again equations (6) and (7) were obeyed qualitatively but D_{eff} was found to be significantly larger than predicted. It now seems likely that multiple scattering was responsible for this, in part, if not wholly (see § 4.3).

3. Experimental, data analysis and results

Several samples of polystyrene spheres were studied but only one is discussed in detail here (see, however, § 5.5). This came from the same preparation as the samples used by Brown *et al* (1975b). The particles had a mean radius of about 250 Å with the standard deviation of the radius being about 19% of the mean. (See § 4.1 and Brown *et al* (1975b) for further discussion of the effects of sample polydispersity.) The sample was prepared in a 1 cm × 1 cm scattering cell containing beads of ion exchange resin using procedures described previously. It stood for 12 days before measurements were made so that the ion exchange resin could remove residual electrolyte and allow the full structure to develop. The concentration was about $1{\cdot}25 \times 10^{-3}$ g cm^{-3}, about 2·5 times larger than the highest concentration used by Brown *et al.*

Light scattering/photon correlation equipment was the same as that used by Brown *et al* except that a more versatile scattering photometer, similar to that described by Pusey *et al* (1974), was used. The 48-channel 'one-bit' correlator was operated in the single-scaled mode (e.g. Jakeman *et al* 1972), where, by contrast with the clipping mode, the quantity c (§ 2.1) does not depend on correlator sample time T. It was therefore possible to link directly measurements made with different sample times to obtain composite correlation functions spanning wide ranges of delay time τ (see e.g. figure 2).

The measurements were made at ambient temperature, $20 \pm 1{\cdot}5$ °C. Experimental results were referred to 20 °C by making the usual (temperature/viscosity) correction to the delay time τ (e.g. Pusey *et al* 1974). Thus, in figures 1, 2 and 4, τ is a corrected time; in figure 3 the diffusion coefficients D_{eff} and D_{L} are similarly corrected to 20 °C.

Figure 1 shows results obtained for 'non-interacting' particles. A dilute sample ($\sim 2\times10^{-4}$ g cm^{-3}) of the 250 Å radius spheres was prepared in a NaCl solution of about 10^{-2} M which should screen the Coulombic interactions effectively. Plots of $\ln(c^{1/2}|g^{(1)}(K,\tau)|)$ against $K^2\tau$ are shown for scattering angles $\theta = 30°$, 90° and 160° ($K = 0{\cdot}886\times10^5$ cm^{-1}, $2{\cdot}42\times10^5$ cm^{-1} and $3{\cdot}37\times10^5$ cm^{-1}). As predicted by equation (4) the data for the three angles are virtually superimposed and lie on a nearly straight line. In fact the solid line in figure 1 is

$$\ln(c^{1/2}|g^{(1)}(K,\tau)|) = -0{\cdot}062 - \bar{D}_0K^2\tau + \tfrac{1}{2}\mu_2\tau^2 \tag{8}$$

where the mean free-particle diffusion coefficient $\bar{D}_0 = 8{\cdot}56\times10^{-8}$ cm^2 s^{-1} and the second cumulant μ_2, which in the absence of particle interactions describes the effect of polydispersity, is given by $\mu_2/(\bar{D}_0K^2)^2 = 0{\cdot}015$. These values are taken from § 4.1 of Brown *et al* (1975b). (Previously, due to an arithmetical error, it was stated erroneously that $\bar{D}_0$ should change by 4% due to polydispersity as K varies from 0 to 3×10^5 cm^{-1}. In fact the effect predicted by equation (20) and table 1 of Brown *et al* (1975b) is less than 1%, no larger than experimental error in figure 1.)

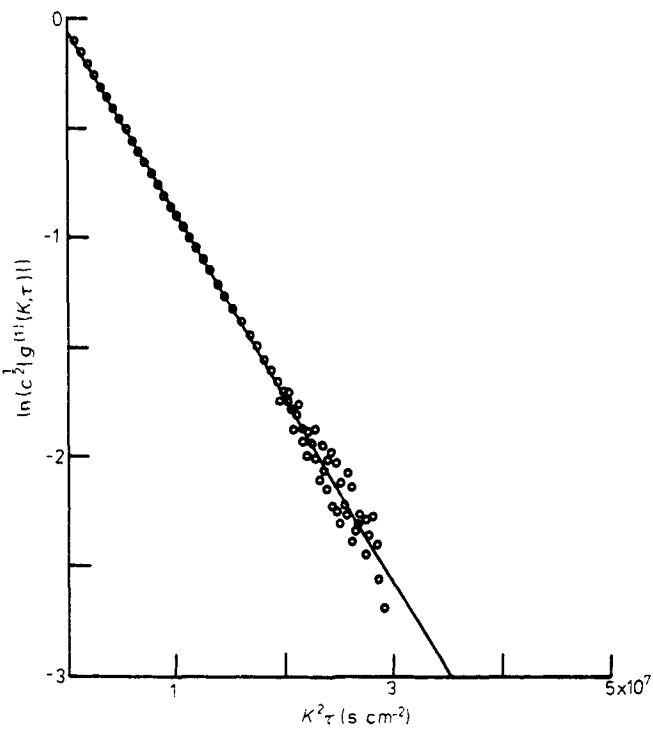

Figure 1. Correlation functions for non-interacting particles at scattering angles $\theta = 30°$, 90° and 160°. For short times the data virtually superimpose and 'representative' data points only are shown. The full line is the 'theoretical' result (see text).

Figure 2 shows correlation functions obtained with the interacting sample for $\theta = 30°$, 76·5° and 140°. For comparison, the full line of figure 1 is reproduced. The effect of the interactions is striking. At short times the data were analysed by the method of moments or cumulants with extrapolation to zero delay time τ, to provide unbiased estimates of c, the effective diffusion coefficient D_{eff} (equation (6)) and the

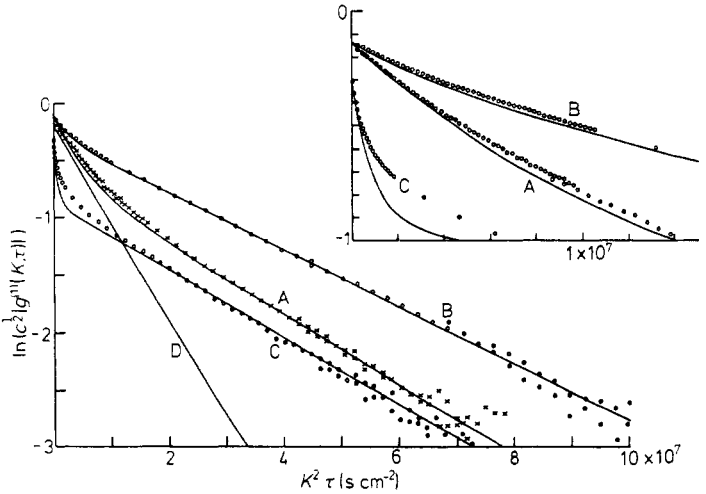

Figure 2. Correlation functions for interacting particles: A, $\theta = 140°$, $K = 3{\cdot}22 \times 10^5$ cm^{-1} ($K > K_{max}$); B, $\theta = 76{\cdot}5°$, $K = 2{\cdot}12 \times 10^5$ cm^{-1} ($K \approx K_{max}$); C, $\theta = 30°$, $K = 0{\cdot}89 \times 10^5$ cm^{-1} ($K \ll K_{max}$).

The free-particle result of figure 1 is reproduced for comparison (curve D). The full curves are obtained from the parameters listed in table 1 using equations (9) and (10). The inset shows the short-time behaviour in more detail.

normalised second cumulant $\mu_2/(D_{eff}\,K^2)^2$ (see e.g. Brown *et al* 1975a or Cummins and Pusey 1977 for further discussion of this extrapolation procedure). In figure 3 D_{eff}^{-1} obtained in this way is plotted against scattering vector K. As predicted by equation (7) this curve has the form of a typical liquid structure factor $S(K)$ with a peak at $K = K_{max} \approx 2{\cdot}04 \times 10^5$ cm^{-1}, $\theta \approx 73°$. The broken line in figure 3 is D_0^{-1}, the result which would be obtained in the absence of particle interactions. Curve A in figure 2 ($\theta = 140°$, $K = 3{\cdot}22 \times 10^5$ cm^{-1}) corresponds to $K > K_{max}$ where $S(K) \sim 1$; the initial slope is thus similar to that for free particles, $D_{eff} \approx D_0$. Curve B ($\theta = 76{\cdot}5°$, $K = 2{\cdot}12 \times 10^5$ cm^{-1}) is for $K \approx K_{max}$; here $D_{eff} < D_0$. For curve C ($\theta = 30°$, $K = 0{\cdot}89 \times 10^5$ cm^{-1}), $K \ll K_{max}$ and $D_{eff} \gg D_0$. Unfortunately, due to the large curvatures in the plots in figure 2, statistical errors in the second cumulants were large: a typical result was $\mu_2/(D_{eff}K^2)^2 = 2 \pm 1$.

It is evident that for all values of K the long-time $K^2\tau$ dependence of $\ln F(K, \tau)$ is roughly linear, implying that $F(K, \tau)$ is quite well described by a single exponential for large enough τ (see § 5.1). The long-time data were analysed as follows: the correlator sample time T was set so that the value of $c^{1/2}|g^{(1)}(K, 48T)|$ was about $e^{-2{\cdot}5}$ to e^{-3}. Then an unweighted (non-linear) four-parameter least-squares fit of the 48 data points representing $c^{1/2}|g^{(1)}(K, \tau)|$ was made to the sum of two exponentials. Provided that the initial and final slopes of the semi-logarithmic plot differed by a factor of two or more, the fitting programme usually converged to a sensible result after a few iterations. The straight parts of the full curves in figure 2 show typical results for the more slowly decaying exponential: clearly the data are adequately represented. The long-time diffusion coefficients D_L obtained from the slopes of these curves are shown in figure 3, where D_L^{-1} is plotted against K. D_L is about three times smaller than D_0 and shows much less K dependence (maximum variation $\sim 30\%$) than D_{eff}. Nevertheless there appears to be a real 'slowing down' of the long-time decay in the region of the peak of $S(K)$.

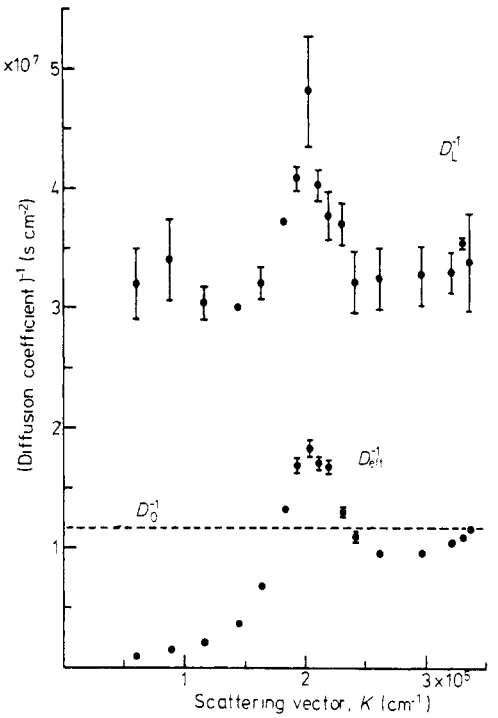

Figure 3. K dependence of the reciprocals of the short-time (D_{eff}, lower curve) and long-time (D_{L}, upper curve) diffusion coefficients. Error bars are standard deviations obtained by performing several experiments under the same conditions. The broken line is D_0^{-1}, the result which would obtain in the absence of interactions.

These two-exponential fits did not, in general, provide a good representation of the short-time data. In particular the values of D_{eff} obtained in this way were invariably lower than those obtained from the cumulants-extrapolation technique outlined above. A factor contributing to this is the limited number of channels in the correlator: when the sample time was chosen so that the long-time behaviour could be investigated, it frequently happened that too few channels covered the short-time behaviour, the initial curvatures in figure 2.

Results of the analysis of the correlation data are given in table 1. We list D_{eff} and c obtained from the short-time cumulant fits and D_{L} and F_{L} obtained from the two-exponential fits, where F_{L} is the fractional strength of the long-time exponential. The curves shown in figure 2 can then be constructed using the equation

$$c^{1/2}|g^{(1)}(K,\tau)| = c^{1/2}[(1-F_{\text{L}})\exp(-D_{\text{S}}K^2\tau)+F_{\text{L}}\exp(-D_{\text{L}}K^2\tau)] \qquad (9)$$

where

$$D_{\text{S}} = \frac{D_{\text{eff}} - F_{\text{L}}D_{\text{L}}}{1-F_{\text{L}}}. \qquad (10)$$

Obviously the initial and final slopes of the experimental correlation functions are well represented by these curves. For intermediate times τ, however, agreement is not so good especially for $K \ll K_{\text{max}}$. Among the reasons for this are the fact that there is no reason *a priori* why the correlation function should be the sum of just two exponentials

Table 1. Compilation of experimental results.

θ (deg)	$K \times 10^{-5}$ (cm^{-1})	$D_{eff} \times 10^{7}$ ($cm^2\ s^{-1}$)	$c^{1/2}$	$D_L \times 10^{7}$ ($cm^2\ s^{-1}$)	F_L	$(D_S K^2)^{-1}$ (μs)
20	0·595	13	0·74	0·32	0·61	87
30	0·886	7	0·74	0·29	0·57	81
40	1·17	4·8	0·76	0·33	0·58	66
50	1·45	2·7	0·80	0·33	0·59	79
57·5	1·64	1·48	0·84	0·31	0·61	112
65	1·84	0·77	0·87	0·27	0·78	116
69	1·94	0·60	0·87	0·25	0·84	107
73	2·04	0·55	0·87	0·21	0·74	160
76·5	2·12	0·59	0·87	0·25	0·87	80
80	2·20	0·60	0·87	0·27	0·80	104
85	2·31	0·77	0·86	0·27	0·65	110
90	2·42	0·92	0·86	0·31	0·65	82
100	2·62	1·05	0·84	0·32	0·62	65
120	2·97	1·05	0·84	0·31	0·58	54
140	3·22	0·96	0·87	0·30	0·61	49
150	3·31	0·93	0·86	0·28	0·56	53
160	3·37	0·87	0·86	0·30	0·61	50

(see, for example, equations (17) and (21), § 5.2). Also the short-time behaviour of the measured correlation functions is probably distorted by multiple scattering (§ 4.3) whose effect is most marked for $K \ll K_{max}$.

4. Sources of experimental uncertainty

4.1. Polydispersity

It should be emphasised that, despite the nearly exponential behaviour of the free-particle correlation functions (figure 1), the sample studied is quite polydisperse, the standard deviation of the radius being about 19% of the mean (§ 3). Although the effects of sample polydispersity on intensity fluctuation spectroscopy measurements in non-interacting systems now appear to be well understood (e.g. Brown *et al* 1975a, Cummins and Pusey 1977) this is not yet the case for interacting systems. Nevertheless it is simple to generalise Pusey's (1975) derivation of equations (6) and (7) to cover polydisperse samples with the result that D_0 in equation (7) is replaced by $\bar{D}_0$, the usual mean diffusion coefficient weighted by the intensity of light scattered by each species. However, the effect of polydispersity on the longer-time behaviour of $F(K, \tau)$ is not so obvious. For the remainder of the paper, therefore, we proceed as if the sample were monodisperse.

Recently a Monte Carlo calculation of van Megen and Snook (1977) produced 'data' for the radial distribution function $g(r)$ similar to the experimental results of Brown *et al* (1975b). Assuming a monodisperse sample, these authors predict that for sample concentrations greater than about $10^{-3}\ g\ cm^{-3}$ the dispersion should have a solid-like arrangement of particles. That this does not appear to be the case for our sample (concentration $\sim 1{\cdot}25 \times 10^{-3}\ g\ cm^{-3}$) may well be due to polydispersity. Indeed Schaefer and Ackerson (1975) have argued that 'charge polydispersity' (and,

presumably, size polydispersity) has the same effect as an impurity in preventing crystallisation.

4.2. Particulate contamination

The presence of particulate contaminants in the sample in intensity fluctuation experiments causes distortion of the measured correlation functions (Cummins and Pusey 1977). The important contaminants are of size about λ or greater. These particles move more slowly than those of the dispersion and their scattering is strongly peaked in the forward direction. Thus the main distortions are expected at long times and at small scattering angles. The presence of particulate contaminants can be detected in several ways: if the photocount flux is measured with an analogue rate meter with integration time of order 10^{-2} to 10^{-1} s, jumpiness of the rate indicates the motion of contaminants through the scattering volume, since the more rapid genuine fluctuations should be integrated out. Similar indications are a jumpy build-up of the correlation function on the oscilloscope display and non-reproducibility of the correlation function from measurement to measurement.

Using these criteria it was found that (as before, Brown *et al* 1975b), immediately after sample preparation, reliable measurements could be made down to $\theta = 20°$. However, after waiting 12 days for the structure to develop, definite indications of particulate contamination were found for $\theta \leqslant 35°$. A contributing factor here is the low intensity ($S(K) \ll 1$) scattered by the structured dispersion at small angles. While measurements of the initial decay were still quite precise, it was harder to obtain accurate long-time measurements and this is reflected in the error bars on D_L^{-1} in figure 3. The source of this particulate contamination has not been determined yet. It may result from residual aggregation of the colloidal particles or from break-up of the ion exchange resin.

It is perhaps worth emphasising that the requirements in these experiments are unusually stringent. We have to make measurements on a 12-day-old, fairly-weak-scattering sample at long correlation delay times and low scattering angles.

4.3. Multiple scattering

The theory outlined in § 2 is based on the first Born approximation. This assumes that the probability is negligible that the light is scattered more than once on passage through the sample. In any light scattering experiment it is obviously important to assess the degree of validity of this assumption. Provided there is no absorption, the presence of multiple scattering is easily detected by measuring the attenuation (due to scattering) of the laser beam transmitted through the sample. For a weak scatterer, the probability p of a single scattering is very much less than 1 and the fractional transmitted intensity T, referred to the direct laser intensity, is roughly $1-p$. If the sample container has approximately equal dimensions in the scattering plane so that the average path lengths traversed in the sample by unscattered and single-scattered light are similar then, in the limit $p \ll 1$, the probability of a double scattering is about p^2. Roughly speaking, then, the relative importance of double scattering compared to single scattering is of the order of p whose magnitude can be obtained from a measurement of T. For our sample $T \approx 0{\cdot}8$, i.e. 80% of the direct laser intensity was transmitted through the sample, and $p \approx 0{\cdot}2$. This implies that double and presumably higher-order multiple scattering must be significant in our experiments.

Recently Sorensen *et al* (1976) have considered, both theoretically and experimentally, the effects of double scattering in a system of *non-interacting* Brownian particles with the assumption of a spherically symmetrical scattering volume. Their theoretical results for particle size very much less than λ, the case for our sample, can be summarised as follows:

(i) The double-scattered intensity is independent of scattering angle (as is the single-scattered intensity for small non-interacting particles).

(ii) The ratio of polarised to depolarised double-scattered intensities is 8, i.e. most of the double-scattered light has the same polarisation as the single-scattered light.

(iii) The initial slope Γ of the field correlation function (as a function of τ) of the double-scattered light is *independent of scattering angle.* Its value is the same as that for single-scattered light at $\theta = 180°$, i.e. $\Gamma = D_0 K_{180}^2$.

(iv) Although this correlation function is not a single exponential, the departure from exponentiality is relatively small (the normalised second cumulant is always less than 0·07).

For several reasons these results cannot be applied directly to our experiments: firstly there are strong interactions in our system; secondly we did not use the spherical scattering volume arrangement considered by Sorensen *et al*; and thirdly higher-order multiple scattering is probably not entirely negligible in our experiment. Nevertheless, lacking an exact theoretical treatment of our situation, it seems likely that these results can at least provide a guide towards estimating the effects of multiple scattering. This conjecture is supported by a few rough measurements on our sample.

In the present experiment the horizontal laser beam was focused in the scattering cell to a diffraction-limited waist of diameter about 200 μm. The sample, when viewed at non-zero scattering angle, showed a bright line (the laser beam profile) due predominantly to single scattering and a more extended diffuse bright region due to multiple scattering. This scattering region was 1 : 1 imaged onto a vertical slit of width a few hundred micrometres and height about 5 mm. Multiple scattering was studied by placing an aperture at the slit which blocked the single-scattered light but accepted multiple-scattered light from a region of height about 1 mm immediately below the laser beam. We found that the intensity of multiple-scattered light showed much less angular dependence than that of the total scattered intensity (single and multiple). If the multiple-scattered intensity was taken as 1 for large θ, $K > K_{max}$, it increased to about 1·6 in the region of the peak and then decreased to about 0·8 for $K \ll K_{max}$. The ratio of multiple-scattered intensity measured in this way to total scattered intensity varied from 4% for $K > K_{max}$ to 2·8% for $K \sim K_{max}$ and around 9% for $K \ll K_{max}$ (where the single-scattered intensity is low). The initial slope of the correlation function was within 20% of its value $\Gamma = D_0 K_{180}^2 \approx 10^4\ s^{-1}$ for single scattering at $\theta = 180°$, for all $20° < \theta < 160°$.

We can now estimate the effects of multiple scattering in our experiments. Firstly the decay time of the correlation function of the multiple-scattered light is rapid compared to the long-time decays in figure 2 for all θ. Thus we expect that the long-time behaviour of the measured correlation functions, the topic of main interest in this paper, will be relatively unaffected by even quite a large amount of multiple-scattered light. Obviously the initial decays will be affected as will the relative intercepts F_L. We can estimate the effect on D_{eff} by writing

$$(D_{eff})_M K^2 = (1-\alpha)(D_{eff})_S K^2 + \alpha\Gamma, \tag{11}$$

where $(D_{\text{eff}})_M$ is the measured value of D_{eff} (including the effect of multiple scattering), $(D_{\text{eff}})_S$ is the value which would obtain in the absence of multiple scattering, α is the fraction of the total intensity which is multiple scattered and $\Gamma = D_0 K_{180}^2 \approx 10^4\ \text{s}^{-1}$. Using estimates for α and the results of table 1 the ratio $(D_{\text{eff}})_S/(D_{\text{eff}})_M$ can be calculated. The results are given in table 2 where we have taken α to have twice the value measured by the method outlined in the previous paragraph in an attempt to allow for the extra intensity of multiple-scattered light arising from the primary scattering volume. Near $\theta = 180°$ there is virtually no effect since $S(K) \sim 1$ and single- and multiple-scattered light have much the same initial decay rate. At and below $K_{\max}$, however, the distortion is significant, 25–35%.

Table 2. The effect of multiple scattering (equation (11)).

θ (deg)	$(D_{\text{eff}})_M \times 10^7$ ($\text{cm}^2\ \text{s}^{-1}$)	$(D_{\text{eff}})_M K^2$ (s^{-1})	α	$\alpha\Gamma$ (s^{-1})	$(D_{\text{eff}})_S K^2$ (s^{-1})	$(D_{\text{eff}})_S \times 10^7$ ($\text{cm}^2\ \text{s}^{-1}$)	$\frac{(D_{\text{eff}})_M}{(D_{\text{eff}})_S}$
160 ($K > K_{\max}$)	0·87	$9{\cdot}90 \times 10^3$	0·080	$0{\cdot}80 \times 10^3$	$9{\cdot}89 \times 10^3$	0·869	1·001
73 ($K \approx K_{\max}$)	0·55	$2{\cdot}28 \times 10^3$	0·056	$0{\cdot}56 \times 10^3$	$1{\cdot}82 \times 10^3$	0·439	1·25
20 ($K \ll K_{\max}$)	13·0	$4{\cdot}60 \times 10^3$	0·180	$1{\cdot}80 \times 10^3$	$3{\cdot}41 \times 10^3$	9·65	1·35

This is a convenient place to make a few other relevant comments on multiple scattering. In our previous measurements (Brown *et al* 1975b) we noted a difference, for $K < K_{\max}$ in the two most concentrated samples, between $S(K)$ obtained by total intensity measurements and D_0/D_{eff}. There this was tentatively attributed to counter-ion–macro-ion interactions which are not considered in the simple theories outlined in § 2. However it now seems more likely that this was a multiple-scattering effect which, for $K < K_{\max}$, increased the measured value of $S(K)$ while decreasing the measured value of D_{eff}^{-1} by the mechanism described above.

As outlined above, the ratio of multiple scattering to single scattering in a light scattering experiment depends on the scattering power of the sample. Provided the peak of the structure factor occurs for θ well below 180°, the scattering power integrated over all θ can, even in the presence of interactions, be estimated from the scattering power assuming no interactions. For particles very much less than λ in size we define a parameter

$$P \equiv \frac{\rho R^6}{\lambda^4}\left(\frac{n_p^2 - n_s^2}{n_p^2 + 2n_s^2}\right)^2 H \tag{12}$$

where ρ is the particle number density, R the particle radius, n_p the refractive index of the particle, n_s the refractive index of the solvent and H is a factor which depends on the experimental arrangement (cell size, scattering geometry etc). Somewhat arbitrarily we assume that, for sample 3 of our previous measurements (Brown *et al* 1975b), the effect of multiple scattering was negligible and thereby obtain a 'maximum permissible' value $P_{\max}$. For this sample $\rho = 2{\cdot}9 \times 10^{12}\ \text{cm}^{-3}$, $R = 250$ Å,

$n_p = 1{\cdot}6$, $n_s = 1{\cdot}33$ and $\lambda = 4880$ Å. Thus

$$P_{max} = 2{\cdot}1 \times 10^{-6} H \text{ cm}^{-1}.$$

For the sample used in the current measurements, $P \sim 7P_{max}$.

For the sample used by Schaefer and Ackerson (1975), $\rho \approx 6{\cdot}4 \times 10^{12}$ cm^{-3}, $R \approx 500$ Å and $\lambda = 6328$ Å giving $P \approx 50P_{max}$. Thus P for their sample was many times greater than both the arbitrary maximum chosen above and the value for the sample used in the current work. Although the simple ideas embodied in equation (11) will not apply exactly to such a strong scatterer, it is clear that, for large enough α, the measured value $(D_{eff})_M$ of the effective diffusion coefficient can be much greater than the true single-scattering value $(D_{eff})_S$. Thus it is possible that the differences between theory (equation (7)) and experiment observed by Schaefer and Ackerson (§ 2.2) are entirely due to multiple scattering.

Finally we note that, with the scattering geometry used in the current experiment (see above) the multiple-scattered light received by the detector originates from a larger volume of the sample than does the single-scattered light. Since the aperture at the detector (~ 600 μm at ~ 70 cm behind the slit) is chosen to accept roughly one coherence area of the single-scattered light, it will accept several coherence areas of the multiple-scattered light. The effect of accepting light over several coherence areas in an intensity fluctuation experiment is to reduce the intercept c of the time-dependent part of the correlation function. This is evident in figure 2 and table 1, the largest effect being for $K \ll K_{max}$ where the fractional multiple-scattered intensity α is largest (table 2). This reduction of intercept can therefore be taken as a further indication of significant multiple scattering. On the other hand, the effect can be minimised by limiting the detection slit in the vertical dimension so that all the light received at the detector originates from the primary scattering volume. Note, however, that this operation should not significantly reduce the distortion of D_{eff} since the multiple-scattered light arising from the primary scattering volume will always mix coherently with the single-scattered light.

5. Discussion

5.1. General comments

Consider first the short-time behaviour of the scattering function $F(K, \tau)$. As has been noted already (§ 3), the plot of D_{eff}^{-1}, obtained from the initial slope of the correlation function, against K (figure 3) has a similar form to that found in previous measurements (Brown *et al* 1975b) which depends on the static structure factor $S(K)$ through equation (7). In fact detailed measurements of the average scattered intensity, and hence $S(K)$, were not made for this sample, since these would have been distorted by multiple scattering as outlined in § 4.3. According to those estimates the lower curve in figure 3 should be shifted upwards by 20 to 30% for $K \leqslant K_{max}$, to obtain true 'single-scattering' results.

For times τ long compared to any characteristic fluctuation time of the particle velocities, i.e. $\tau \gg \tau_I$, quite general memory-function arguments (e.g. Pusey 1975) predict that $F(K, \tau)$ should decay exponentially. This prediction is supported by the linear trends in the semi-logarithmic plots of figure 2. An estimate of the fluctuation time τ_I is the decay time $(D_S K^2)^{-1}$ of the faster-decaying exponential in a two-exponential representation $F(K, \tau)$ (equations (9) and (10)). Values of this quantity

(table 1) range from around $0{\cdot}5\times10^{-4}$ s to about $1{\cdot}2\times10^{-4}$ s, and show relatively little K dependence. These two observations give qualitative support to the concept and properties of an 'interaction' component of particle velocity as discussed in § 2.

5.2. Single-particle motions

Further insight into the nature of the particle motions can be obtained by adapting some of the theory of neutron scattering by atomic liquids (see, for example, Sjölander 1965). We write equation (2) in the form

$$F(K,\tau)=N^{-1}\sum_{i=1}^{N}\langle\exp[\mathrm{i}\boldsymbol{K}\cdot(\boldsymbol{r}_i(0)-\boldsymbol{r}_i(\tau))]\rangle+N^{-1}\sum_{\substack{i=1\\ i\neq j}}^{N}\sum_{j=1}^{N}\langle\exp[\mathrm{i}\boldsymbol{K}\cdot(\boldsymbol{r}_i(0)-\boldsymbol{r}_j(\tau))]\rangle$$

$$\equiv F_{\mathrm{S}}(K,\tau)+F_{\mathrm{D}}(K,\tau), \tag{13}$$

where the self-intermediate-scattering function $F_{\mathrm{S}}(K,\tau)$ describes single-particle motions whereas the distinct term $F_{\mathrm{D}}(K,\tau)$ depends on the correlated motions of different particles. In neutron scattering, by using both coherent and incoherent techniques, it is frequently possible to measure both $F(K,\tau)$ and $F_{\mathrm{S}}(K,\tau)$ thereby separating the single-particle and many-particle functions. Unfortunately the light scattering method used in the present work is intrinsically coherent providing only the full function $F(K,\tau)$. However the $\tau=0$ limit of equation (13),

$$S(K)=1+F_{\mathrm{D}}(K,0), \tag{14}$$

shows that the departure of $S(K)$ from unity is a measure of the importance of the many-particle terms. Thus, for $K>K_{\max}$, where $S(K)\sim1$, a measurement of $F(K,\tau)$ can be taken as an estimate of $F_{\mathrm{S}}(K,T)$ since it seems unlikely that, if $F_{\mathrm{D}}(K,0)$ is small, $F_{\mathrm{D}}(K,\tau)$ would be significant.

By definition (equation (13)),

$$F_{\mathrm{S}}(K,\tau)=N^{-1}\sum_{i=1}^{N}\langle\exp[\mathrm{i}\boldsymbol{K}\cdot(\boldsymbol{r}_i(0)-\boldsymbol{r}_i(\tau))]\rangle=\langle\exp(-\mathrm{i}\boldsymbol{K}\cdot\Delta\boldsymbol{R}(\tau))\rangle \tag{15}$$

where we have assumed the particles to be identical and the particle displacement $\Delta\boldsymbol{R}(\tau)$ is defined by

$$\Delta\boldsymbol{R}(\tau)\equiv\boldsymbol{r}(\tau)-\boldsymbol{r}(0)\equiv\int_0^{\tau}\boldsymbol{V}(t)\,\mathrm{d}t, \tag{16}$$

$\boldsymbol{V}(t)$ being the instantaneous particle velocity. We now assume $\Delta\boldsymbol{R}(\tau)$ to be a Gaussian-distributed random variable. This is certainly a valid assumption for $\tau_{\mathrm{B}}\ll\tau\ll\tau_{\mathrm{I}}$ where free-particle Brownian motion dominates and also for times τ much greater than the maximum velocity fluctuation time τ_{I}. Its validity is questionable for $\tau\approx\tau_{\mathrm{I}}$. With this assumption, equation (15) becomes

$$F_{\mathrm{S}}(K,\tau)=\exp(-\tfrac{1}{6}K^2\langle\Delta R^2(\tau)\rangle), \tag{17}$$

where, from equation (16), the mean-square displacement is given by

$$\langle\Delta R^2(\tau)\rangle=\int_0^{\tau}\int_0^{\tau}\langle\boldsymbol{V}(t)\cdot\boldsymbol{V}(t')\rangle\,\mathrm{d}t\,\mathrm{d}t'. \tag{18}$$

which can be written (e.g. Berne and Pecora 1976, p 84)

$$\langle \Delta R^2(\tau) \rangle = 2 \int_0^\tau (\tau - t) \langle \boldsymbol{V}(0) \cdot \boldsymbol{V}(t) \rangle \, \mathrm{d}t. \tag{19}$$

To proceed further we model the velocity autocorrelation function as follows:

$$\langle \boldsymbol{V}(0) \cdot \boldsymbol{V}(t) \rangle = 6D_0 \delta(t) - 3A \exp(-t/\tau_I). \tag{20}$$

The first term represents the Brownian components of velocity which fluctuate fast enough ($\tau_B \approx 10^{-10}$ s) that the explicit form of its τ dependence is unimportant and can be expressed by the Dirac δ function. The second term represents the interaction components of velocity. A is a positive parameter and the negative sign is chosen *a posteriori* to fit the data (see below). The exponential form for this term is chosen simply for convenience. Substitution of (20) in (19) gives

$$\tfrac{1}{6}\langle \Delta R^2(\tau) \rangle = D_0 \tau - A\tau_I[\tau + \tau_I \exp(-\tau/\tau_I) - \tau_I]. \tag{21}$$

For $\tau \ll \tau_I$,

$$\langle \Delta R^2(\tau) \rangle = 6D_0 \tau, \tag{22}$$

the usual result for free-particle Brownian motion. For $\tau \gg \tau_I$,

$$\tfrac{1}{6}\langle \Delta R^2(\tau) \rangle = D_0 \tau - A\tau_I \tau + A\tau_I^2. \tag{23}$$

Substitution of (23) into (17) gives

$$F_S(K, \tau)|_{\tau \gg \tau_I} = \exp[-(D_0 - A\tau_I)K^2 \tau] \exp(-AK^2 \tau_I^2). \tag{24}$$

Comparison of (24) with (9) and (1) shows that, for $K > K_{max}$ ($S(K) \sim 1$) and $\tau \gg \tau_I$, the identifications

$$D_L = D_0 - A\tau_I, \tag{25}$$

$$F_L = \exp(-AK^2 \tau_I^2) \tag{26}$$

can be made.

In figure 4, $-6 \ln|g^{(1)}(K, \tau)|/K^2$ is plotted against τ for $K = 3{\cdot}37 \times 10^5$ cm^{-1} ($S(K) \sim 0{\cdot}99$) and $K = 2{\cdot}42 \times 10^5$ cm^{-1} ($S(K) \sim 0{\cdot}94$). Since $S(K) \sim 1$, the arguments given in the first paragraph of this section imply that this quantity should be an estimate of $\langle \Delta R^2(\tau) \rangle$. The data for the two values of K do not superimpose perfectly, perhaps because of the 6% contribution from the distinct term for $K = 2{\cdot}42 \times 10^5$ cm^{-1}. The full curve in figure 4 is equation (21) with parameters $A = 5{\cdot}48 \times 10^{-4}$ cm^2 s^{-2} and $\tau_I = 103$ μs, roughly the mean values for the two sets of data obtained from equations (25) and (26) and table 1 ($D_0 = 0{\cdot}856 \times 10^{-7}$ cm^2 s^{-1}, § 3). There is quite reasonable agreement between experiment and theory despite the many assumptions involved in this comparison.

Thus, as with dense simple liquids, there appears to be a weak but long-lived negative part to the velocity autocorrelation function of a single particle (equation (20)). A particle can be thought of as temporarily trapped in a repulsive cage formed by its nearest neighbours. Due to motions of these neighbours, the cage is continuously evolving, only maintaining a given configuration for about one collision time τ_I. For times much longer than τ_I, a particle 'random-walks' through the dispersion with a self-diffusion coefficient D_L several times smaller than that which would obtain in the absence of interparticle interactions. Obviously, from dimensional considerations alone, the quantity A can be identified with $\langle V_I^2 \rangle$, the mean-square value of the

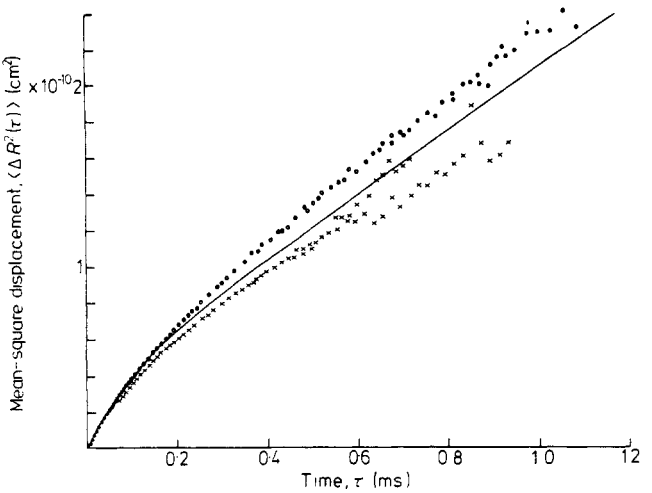

Figure 4. Mean-square displacement of a particle as a function of time. The full curve is equation (21) with values of the parameters as given in the text. The upper set of experimental data is for $K = 2{\cdot}42 \times 10^5\ \mathrm{cm}^{-1}$ ($S(K) \approx 0{\cdot}94$) and the lower set for $K = 3{\cdot}37 \times 10^5\ \mathrm{cm}^{-1}$ ($S(K) \approx 0{\cdot}99$). For $\tau \lesssim 0{\cdot}1$ ms the two sets of data superimpose.

interaction component of particle velocity. It is gratifying that the values of $\langle V_I^2 \rangle \approx 5{\cdot}5 \times 10^{-4}\ \mathrm{cm}^2\ \mathrm{s}^{-2}$ and $\tau_I \approx 100\ \mu\mathrm{s}$ which describe the present data are not too different from previous very rough theoretical estimates, $3 \times 10^{-4}\ \mathrm{cm}^2\ \mathrm{s}^{-2}$ and 200 μs respectively (Pusey 1975).

5.3. Cooperative motions

As with simple liquids, it is quite difficult to obtain even a qualitative feel for the full behaviour of the coherent scattering function $F(K, \tau)$ in our system. Here we simply note that the values obtained for D_L (table 1) for $K < K_{max}$, where correlated motions are important, are similar to those for $K > K_{max}$ where single-particle motions dominate (§ 5.2). This suggests that the 'Vineyard' approximation (e.g. Sjölander 1965, p 321),

$$F(K, \tau) = S(K) F_S(K, \tau) \tag{27}$$

might apply for $\tau \gg \tau_I$ although it clearly does not describe the short-time data. It is, in fact, for long times that this approximation is most likely to be valid. However, the 'Vineyard' approximation has not been too successful in describing the behaviour of simple liquids and it would obviously be prudent to obtain more results on Brownian systems before pursuing this approach seriously. In addition, it is not clear how the peak in D_L^{-1} (figure 3), if it is real, can be reconciled with equation (27).

5.4. Other theories

There have been several theoretical treatments of Brownian motion in interacting systems based on N-particle diffusion equations which start more or less from first principles (e.g. Murphy and Aguirre 1972, Altenberger and Deutch 1973, Phillies

1974, Altenberger 1974, 1976, Ackerson 1976, Hess and Klein 1976). At present, however, to make predictions from these theories which apply to specific experiments it is still necessary to make approximations such as linearisation of the equations or restrictions to weak interactions. It thus appears that none of these theories can yet be applied to the current experiments. However, it is hoped that the data presented here may stimulate further theoretical progress.

The theory of this type which, at present, comes closest to being directly useful is that of Ackerson (1976) who, in addition to deriving the result of equations (6) and (7), also obtained a result for the second cumulant, μ_2, in terms of the interparticle potential. Unfortunately, in the present work, it was not possible to obtain reliable values of μ_2, both for the reasons mentioned in § 3 and because of the distorting effect of multiple scattering at short times (§ 4.3). Nevertheless, Ackerson (1977) has analysed earlier data in terms of this theory. He was also able to estimate the effects of hydrodynamic interactions and the counter-ion clouds.

Berne (1977) has formulated a heuristic model for interacting Brownian particles based on a memory-function approach. This gives the correlation function $F(K, \tau)$ as the sum of two exponentials as well as predicting the result of equations (6) and (7). It was a simple matter to convert the parameters of the data given in table 1 into the parameters of Berne's theory. However, it was not immediately obvious that this conversion provided additional insight into the problem and, in the limited space available here, we will not discuss this comparison further. Berne (1977) has also applied a mode–mode coupling approach to the problem.

5.5. Other samples

Measurements were also made on a more dilute sample of the same spheres. Its concentration ($\sim 5 \times 10^{-4}$ g cm^{-3}) was about the same as the most concentrated sample studied by Brown *et al* (1975b) and the peak in $S(K)$ was at $\theta \sim 50°$. The results obtained were qualitatively the same as with the first sample giving further confirmation that the effects of multiple scattering have not seriously affected the conclusions of this paper. The most noteworthy difference concerned the magnitude of D_L which overall was about 10% higher, presumably reflecting decreased hindering of the particle motions in the more dilute sample. On further dilution (so that K_{max} decreases) it became impossible to make meaningful long-time measurements for $K < K_{max}$ because of the effects of particulate contamination at small angles (§ 4.2).

Acknowledgments

This work is part of a continuing collaboration with R H Ottewill and J W Goodwin of Bristol University. I am grateful to them for providing the samples and for many valuable discussions.

Note added in proof. It is worth mentioning that more justification can be given for the form of velocity autocorrelation function assumed in equation (20). As a first approximation one might take the potential experienced by a particle in its instantaneous repulsive cage to be harmonic. The velocity autocorrelation function for a harmonically-bound Brownian particle is given by equation (50*c*) of the classic paper by Wang and Uhlenbeck (1945). In the strongly overdamped case it consists of

the sum of a positive, large-amplitude, rapidly-decaying exponential due to the solvent molecules (modelled by the δ function in (20)) and a *negative*, small-amplitude, slowly-decaying exponential representing the effect of the potential. It seems plausible that evolution of the cage, not treated by Wang and Uhlenbeck, will decrease somewhat the time constant of the negative exponential, but that the general form assumed for equation (20) is a sensible first guess. This 'diffusing particle in a diffusing cage' model has also been considered by A Bøe and P Dalberg (private communication). I am grateful to Dr Bøe for correspondence on this point as well as valuable general criticism of the paper.

Another reference relevant to § 2.2, not to hand when this paper was submitted, is Schaefer (1977).

References

Ackerson B J 1976 *J. Chem. Phys.* **64** 242–6

—— 1977 *Photon Correlation Spectroscopy and Velocimetry* eds H Z Cummins and E R Pike (New York: Plenum) pp 440–3

Altenberger A R 1974 *Acta Phys. Pol.* A **46** 661–6

—— 1976 *Chem. Phys.* **15** 269–77

Altenberger A R and Deutch J M 1973 *J. Chem. Phys.* **59** 894–8

Berne B J 1977 *Photon Correlation Spectroscopy and Velocimetry* eds H Z Cummins and E R Pike (New York: Plenum) pp 344–85

Berne B J and Pecora R 1976 *Dynamic Light Scattering* (New York: Wiley)

Brown J C, Pusey P N and Dietz R 1975a *J. Chem. Phys.* **62** 1136–44

Brown J C, Pusey P N, Goodwin J W and Ottewill R H 1975b *J. Phys. A: Math. Gen.* **8** 664–82

Cummins H Z and Pusey P N 1977 *Photon Correlation Spectroscopy and Velocimetry* eds H Z Cummins and E R Pike (New York: Plenum) pp 164–99

Harris S 1976 *J. Phys. A: Math. Gen.* **9** 1093–100

Hess W and Klein R 1976 *Physica* A **85** 509–27

Jakeman E, Oliver C J, Pike E R and Pusey P N 1972 *J. Phys. A: Gen. Phys.* **5** L93–6

van Megen W and Snook I 1977 *J. Chem. Phys.* **66** 813–7

Murphy T J and Aguirre J L 1972 *J. Chem. Phys.* **57** 2098–104

Phillies G D J 1974 *J. Chem. Phys.* **60** 976–82

Pusey P N 1975 *J. Phys. A: Math. Gen.* **8** 1433–40

Pusey P N, Koppel D E, Schaefer D W, Camerini-Otero R D and Koenig S H 1974 *Biochemistry* **13** 952–60

Pusey P N, Schaefer D W, Koppel D E, Camerini-Otero R D and Franklin R M 1972 *J. Physique Coll.* **33** C1 163–8

Schaefer D W 1977 *J. Chem. Phys.* **66** 3980–4

Schaefer D W and Ackerson B J 1975 *Phys. Rev. Lett.* **35** 1448–51

Schaefer D W and Berne B J 1974 *Phys. Rev. Lett.* **32** 1110–3

Sjölander A 1965 *Thermal Neutron Scattering* ed P A Egelstaff (London: Academic) pp 291–345

Sorensen C M, Mockler R C and O'Sullivan W J 1976 *Phys. Rev.* A **14** 1520–32

Wang M C and Uhlenbeck G E 1945 *Rev. Mod. Phys.* **17** 323